

A Photovoltaic Cell Defect Detection Method Using Electroluminescent and Googlenet

Binhui Liu¹, Qiangrong Yang¹, Yurong Han²

¹Quality Inspection and Testing Center, The Fifth Institute of MIIT

²Pony.ai

Keywords: Photovoltaic cell defect detection, Convolutional Neural Network CNN, Electroluminescent (EL), GoogLeNet

Abstract: Electroluminescent (EL) plays an important role in the application of photovoltaic cell Defect detection. Traditional approaches for EL result analysis usually utilize visual inspection by technicians and have the drawbacks of low efficiency which can be improved by employing deep convolutional neural network (CNN) features that contain more semantic and structure information and thus possess more discriminative ability. Therefore, a defect detection method based on EL and GoogLeNet is proposed in this work. Firstly, a database of EL image samples for photovoltaic cell defects is built, then a deep convolutional neural network based on GoogLeNet is established. At last, the experiments and simulation tests prove that the presented defect detection approach is superior to the conventional methods. The detection precision is more than 85%, while the previous accuracy is under 67%. What's more, the proposed method is more stable and efficient.

1. Introduction

Photovoltaic (PV) cell obtains extensive attention around the world as an environmental energy resource and the photovoltaic cell industry gets rapid development [1][2]. Nowadays, the domestic scale of solar cell industry is expanding. In the production process, there are many factors that easily cause cell defects, such as the fault in material and manufacture damage. These defects lead to some problems in modules, which directly impacts cells' transfer efficiency and service life [3].

Electroluminescent (EL) test plays an important role in quality and process management [4] [5]. It is a common technique for defect detection in photovoltaic industry due to the advantages including simple operation, low cost, better repeatability and fast detection speed. The EL devices have been able to conduct automatic test and the test sampling period approaches 3 seconds. In traditional practices, the results analysis of EL test is completed by technicians. However, the defect situations of photovoltaic cell are multifarious and the defect types are more than a dozen, which makes it difficult for analysis. In this case, the test accuracy rate of a technician is less than 70% and it will decrease when the visual inspection leads to visual fatigue. Therefore, other result analysis methods should be employed to increase the precision.

With the rapid development of Artificial Intelligence (AI) image recognition, the relevant techniques have been applied to many fields. Deep learning possesses the powerful ability of input data feature extraction because it can form more abstractive and high-level feature representation by combining and studying low-level data. In the image application, deep learning can decrease the error rate to 1.2% in MINST recognition [6]. In 2012, the Alex-Net [7] model achieves a great success on the ImageNet competition with 10% higher accuracy than other state-of-the-art methods. GoogLeNet [8] is a well-known trained CNN implementation that uses ImageNet and it can attain a low error when trained over the millions of images contained in ImageNet. GoogLeNet is often used in photo classification, as a large fraction of examples in ImageNet are composed of photos. In this case, it can generalize well and successfully classify out-of-sample examples. In conclusion, to improve the detection efficiency based on EL test, image recognition technology based on

GoogLeNet is employed in photovoltaic cell defect detection. Compared to traditional method, it can realize higher intelligence, more convenient integration and lower manufacturing cost.

To overcome the disadvantages of traditional approach for EL test result analysis and inspired by the studies in image recognition using deep learning, we argue that it is more appropriate to employ image recognition method using deep learning than visual inspection for photovoltaic cell defect detection. Furthermore, the training model is the CNN base on GoogLeNet whose conventional network structure is easily engineered and practically promoted.

The rest of this paper is organized as follows. Section 2 gives introductions of EL test and CNN based on GoogLeNet. In Section 3, the principle of the proposed defect detection method is detailed. The experimental settings and results are described in Section 4 with the performance of the proposed method presented and compared with the conventional method. At last, Section 6 concludes this work and figures out several future research prospects.

2. Brief Introductions of EL and GoogLeNet

2.1 EL Test in photovoltaic cell defect detection

The principle of EL test in photovoltaic cell defect detection is that when a photovoltaic cell is electrifying positively, the electron and hole recombination releases power by emergent photon and an electroluminescent spectrum with 700-1200 nm wavelength is formed. Then the defect part of photovoltaic cell will appear obvious macula due to the lack of electron and hole recombination. When Charge-Coupled Device (CCD) Type is applied to capture the image, different defect types present respective EL images with specific features. The EL test system is shown in Fig. 1.

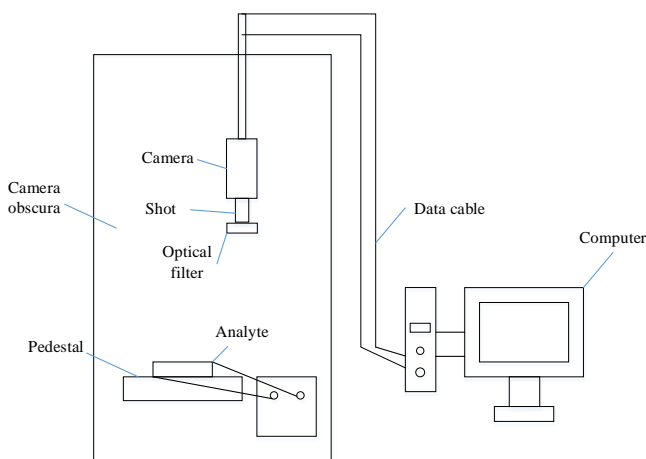
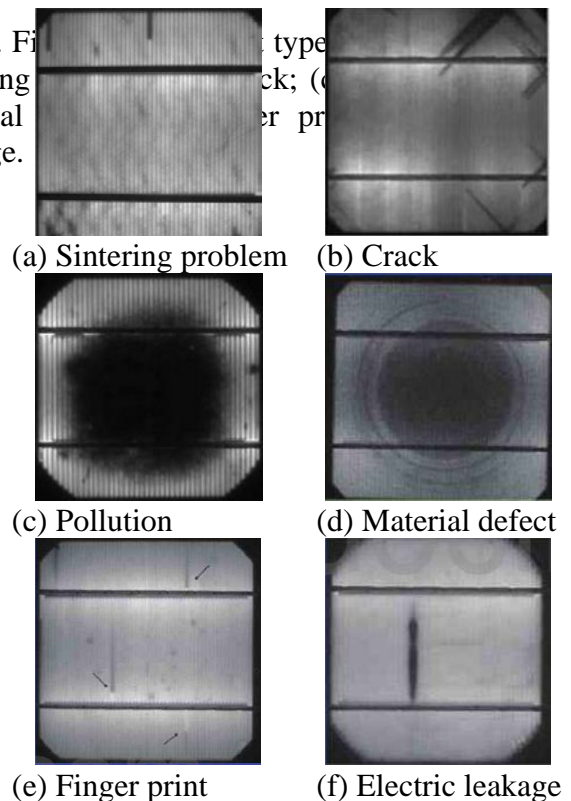


Fig. 1. EL test system

Fig. 2. Five types of defects: (a) sintering problem; (b) crack; (c) pollution; (d) material defect; (e) finger print; (f) electric leakage.



Different defect types result in different images with disparate features. Fig. 2 lists the figure results that are corresponding to several typical types of cell defects.

3. CNN based on GoogLeNet

There are two main kinds of deep learning model, one is Deep Belief Network (DBN) and the other is Convolutional Neural Network (CNN). GoogLeNet is a recent deep CNN model developed by Google. One significant characteristic of GoogLeNet is that it is designed very deep, while the network is 22 layers deep when counting only layers with parameters (or 27 layers if also count pooling layers). Another characteristic of GoogLeNet is that a new local Inception module was introduced to CNN. The basic idea of Inception module is to find the optimal local construction and to repeat it spatially. One of the main beneficial aspects of this architecture is that it allows for increasing the number of units at each stage significantly without an uncontrolled blow-up in computational complexity. So that the CNN can be designed not only very deeply but also be efficiently trainable.

The network structure of GoogLeNet is consist of four main modules:

3.1 Convolution

Convolution module contains input and convolutional kernel. There are several feature planes in the module. Each feature plane is formed by some regular arranged neurons and the neurons in a plane own the same weight value which is convolutional kernel, namely. Convolutional kernel is usually initialized by a random decimal matrix, then it would acquire reasonable weight value during network training period. The direct benefit is to reduce the connection between network layers and the risk of overfitting is lowered as well.

3.2 Pooling

Pooling layer divides a convolutional region into sub regions. The purpose is to reduce the computational time of subsequent layers and increase the robustness of the feature with respect to its spatial position.

There are two common types: max pooling and average pooling, and the two down sampling can be seen as special convolution processes. If the input figure is represented as X:

Each weight value in average pooling is 0.25, the sliding size of convolutional kernel is 2. In this case, the figure is obscured to 25% percent of the original one.

In max pooling, there is only one weight in a convolutional kernel is set to 1 and the others are set to 0. The grid whose weight is 1 in the convolutional kernel is corresponding to the grid with the maximum value in the region covered by the convolutional kernel in figure X. When the sliding size is 2, the operation shrinks the original figure to 25% but remain the maximum input data within a 2*2 area.

3.3 Softmax

To avoid gradient vanishing, the network should add two auxiliary softmax layers to transmit gradient forwards. Besides, the two category modules should be assisted an attenuation coefficient and the effect is decreasing with increasing iteration number.

3.4 Others

Other modules mainly contain depth content and local response normalization. The function of these modules is to integrate the feature figures with different depth and regularize partial response, then improve the prediction precision.

4. Defect detection method based on El Test and GoogLeNet

4.1 Training set of photovoltaic cell defect detection samples

There are several kinds of defect types:

4.2 Process problems

Process problems depict incorrect operations caused by man or machines during manufacturing process marked with yellow dash-line in Fig.3. Defects in the figure are occurred in cleaning process, coating process, etching process, sintering process, contamination process and doping process, respectively.

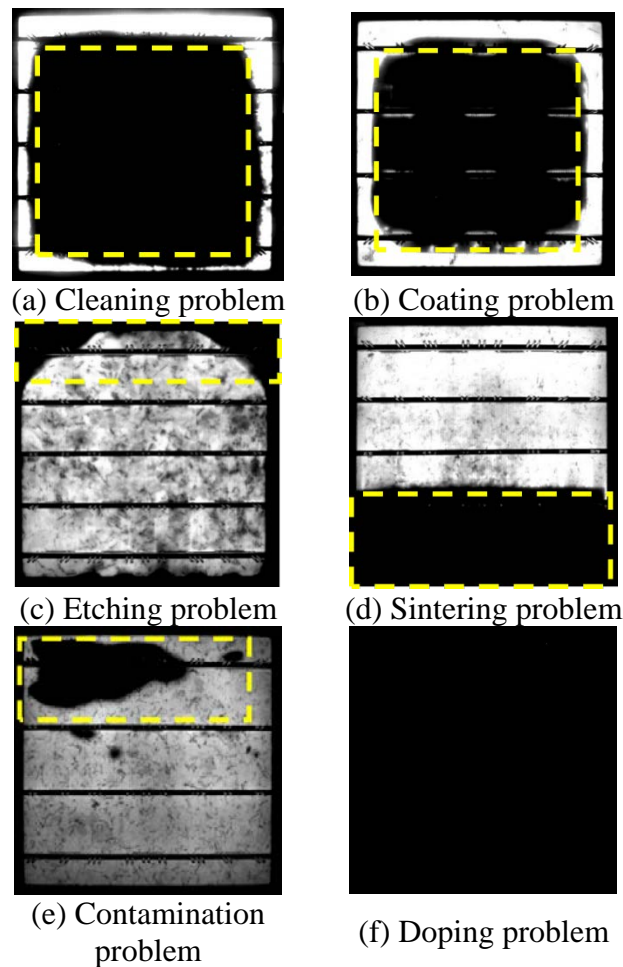


Fig.3. Figures of different types of defects scribed to manufacturing process:

(a) Cleaning problem (b) coating problem (c) etching problem (d) sintering problem (e) contamination (f) doping problem.

4.3 Scratch problems

Scratch problems are usually consisted with micro crack (non-visible), deep cracks and edge breakage marked with yellow dash-line in Fig 4.

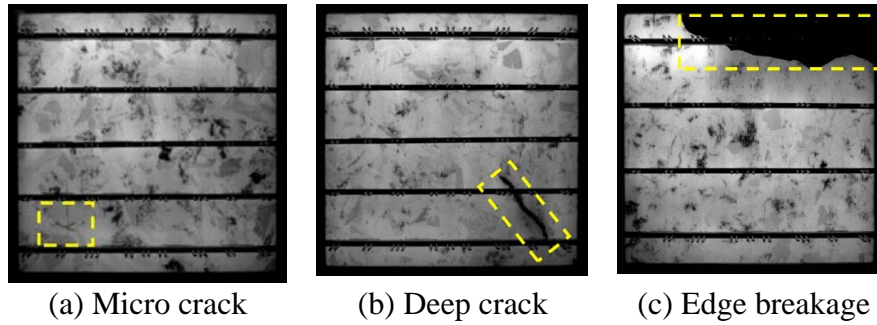


Fig. 4. Figures of different scratch types: (a) micro crack (b) deep crack (c) edge breakage.

4.4 Material problems

Material problems are usually caused by the excessive content of impurities in bulk materials or grain boundaries, which leads to a sharp decrease in minority carrier lifetime at corresponding sites.

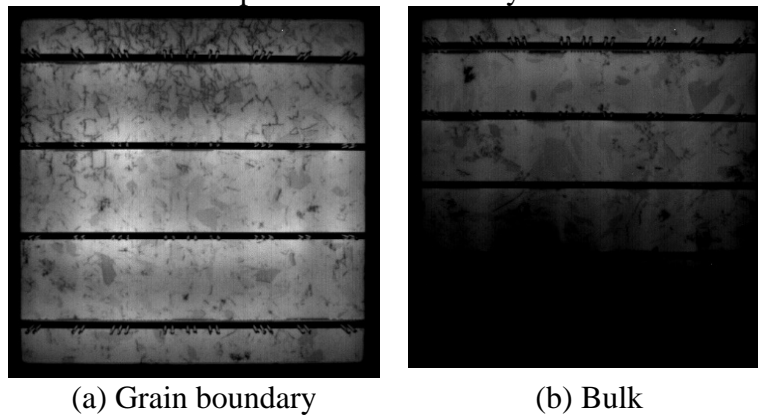


Fig.5 Material problems caused by excessive content of impurities: (a) grain boundary (b)bulk.

5. Methodology

5.1 Support Vector Machine (SVM)

SVMs is a common approach for classification. [11] Firstly, local descriptors are employed to describe the features typically extracted at salient points in segmented PV cells images. Moreover, the – salient points are, also known as key points, or from dense pixel grids. To train the classifier and subsequent predictions, a global representation needs to be computed from the set of local descriptors, oftentimes referred to as encoding. Finally, this global descriptor for a solar cell is classified into defective or functional.

The locations of these local features are determined by two sampling strategies: key point detection and dense sampling. On one hand, key point detection automatically determines salient points for feature descriptors. The number of detected key points varies greatly with the image content (and parameters) determined by the amount of high frequencies in the image. Key point detectors typically operate in scale space, allowing feature detection at different scale levels. On the other hand, dense sampling subdivides the 300X300 pixels PV cell by overlaying it with a grid consisting of $n \times n$ cells. The center of each grid cell specifies the position at which a feature descriptor will be subsequently extracted. In contrast to keypoint detectors, the number of feature locations does not vary with the image content, but only depend on the grid size in the dense sampling.

Then, SVMs are trained with a linear and a Radial Basis Function (RBF) kernel. Liblinear [12], optimized by linear classification tasks and large datasets, is used as linear kernel, and Libsvm [13] is the nonlinear RBF kernel.

The SVM hyperparameters are determined by evaluating the average F1 score in an inner fivefold cross-validation on the training set using a grid search. For the linear SVM, we employ the Γ^2

penalty on a squared hinge loss. The penalty parameter C is selected from a set of powers of ten, i.e., $C_{\text{linear}} \in \{10^k | k=-2, \dots, 6\}$. For RBFSVMs, the penalty parameter C is determined from a slightly smaller set $C_{\text{RBF}} \in \{10^k | k=2, \dots, 6\}$ the search space of the kernel coefficient is constrained to $\gamma \in \{10^{-7}, 10^{-6}, S^{-1}\} \subset [0, 1]$ where S denotes the number of training samples.

5.2 Deep CNN

Several strategies are considered to train the CNN. Given the amount of data we had at our disposal is limited, best results were achieved by averaging the transfer learning. GoogLeNet [14] is utilized as network architecture originally trained on the ImageNet dataset [15] using 1.28 million images and 1,000 classes, then the network is refined using the dataset.

The two fully connected layers of GoogLeNet are replaced by a Global Average Pooling (GAP) [16] and two fully connected layers with 4,096 and 2,048 neurons, respectively. The GAP layer is used to make the GoogLeNet network input tensor ($224 \times 224 \times 3$) be compatible to the resolution of our solar cell image samples ($300 \times 300 \times 3$), in case of additional own sampling of the samples. The output layer is consisting of a single neuron and outputs the defect probability of a cell. The CNN is refined by minimizing the Mean Squared Error (MSE) loss function. Hereby, a deep regression network is trained essentially to predict (continuous) defect probabilities trained using four defect likelihood categories (functional, man problem, material problem and scratch problem). At last, we can directly compare CNN decisions against the original ground truth labels without binarizing them by rounding the predicted continuous probability to the nearest neighbor of the four original classes.

Data augmentation is employed to generate additional and slightly perturbed training samples. The augmentation variability, however, is kept moderate, since the segmented cells vary only by few pixels along the translational axes and few degrees along the axis of rotation. The training samples are scaled by almost 2% of the original resolution.

We fine-tune the pre-trained model in two stages. Firstly, we only train the fully connected layers while keeping the weights of the convolutional blocks fixed. Here, we employ the Adam optimizer [17] with a learning rate of 10^{-3} , exponential decay rates $\beta_1 = 0.9$ and $\beta_2 = 0.999$, and the regularization value $\epsilon = 10^{-8}$. In the second step, we refine the weights of all layers. At this stage, we use the Stochastic Gradient Descent (SGD) optimizer with a learning rate of 5×10^{-4} and a momentum of 0.9.

In both stages, we process the augmented versions of the 11376 training samples in mini-batches of 360 samples on a desktop of core i5 3.3G Hz, 8G RAM and 1T hardware, and run the training procedure for a maximum of 500 epochs. For the implementation of the deep regression network, we use Anaconda version 3.3.1 with TensorFlow version 1.2.1 [18] in the backend.

6. Experiments and analysis

6.1 Datasets

The dataset we used in this paper is extracted from high resolution EL from a co-operated solar cell manufacturing company. The EL images were captured in a dark room using a camera placed on a tripod. A controlled environment for taking EL images was necessary due to a long exposure time required for image acquisition. This especially stems from the fact that the amount of radiation emitted by PV modules is comparatively low opposed to background radiation on an average day.

In total, we extracted 11376 solar cells from the high resolution EL and the extracted solar cells exhibit intrinsic and extrinsic defects. Particularly, the dataset includes micro and deep cracks, short-circuited cells, open inter-connects, and soldering failures. These cell defects are widely known to negatively influence efficiency, reliability, and durability of solar modules. Finger interruptions are excluded since the power loss caused by such defects is typically negligible.

6.2 Performance

In the experiments, all the extracted solar cell images are divided into training sets and validation sets (9000 images in training set and 2376 images in validation set). Then the training sets are fed to train the SVM model and deep CNN model, and the validation set is used to validate the trained models. The performance of the two models is shown in Fig.6.

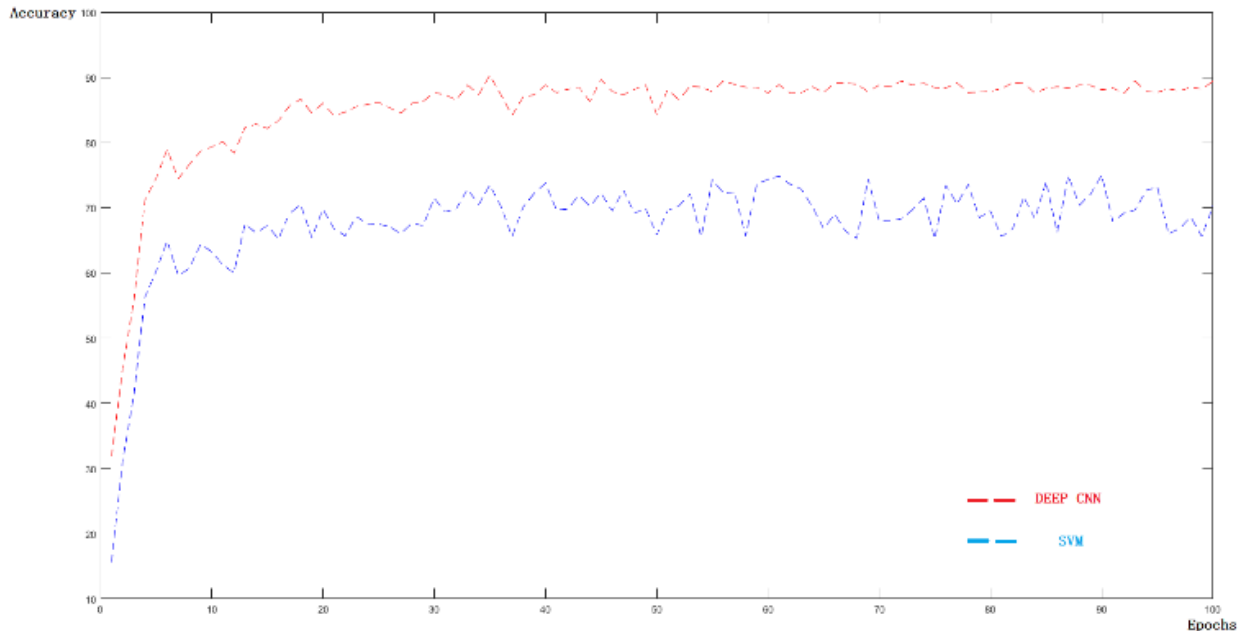


Fig.6. Performances of two models

It is figured out that the performance of our deep CNN method outperforms the SVM method. The accuracy of the deep CNN method is 88.7%, while the accuracy of the SVM method is 67%. Moreover, our method converges within about 30 epochs while the SVM method took 45 epochs to reach the optimal value. The confusion matrix is shown in Table I.

Table 1. The confusion matrix

	Man problem	Scratch problem	Material Problem
Man problem	93	6	14
Scratch problem	6	105	5
Material Problem	28	6	108

In the table, it shows that our method performs well since most of the defected solar cells are classified correctly. However, some defect types of material problem are usually classified as man problems. The hypothetic reason for above mistake is that man problems contain 6 types of defects in which material defects are likely to occur simultaneously, which leads the division of material defects into human causes.

7. Conclusion

Electroluminescent (EL) is the main technique for photovoltaic cell Defect detection. To improve the efficiency of EL result analysis, a defect detection method based on CNN is proposed in the paper. GoogLeNet is one of the prime CNN models for vision computing owing to its less neurons, small-scale parameters, low model complexity and outstanding performances. The effectiveness of the proposed method is verified by a series of experiments, and the results demonstrate that the proposed model has better performances than the original detection approach depending on visual inspection by technician. In the future, we will investigate the possibility of employing other CNN models in this application or utilizing the GoogLeNet models in other similar application.

Acknowledgements

This work was supported by Industrial Internet Innovation and Development Project “Ceprei Cloud” Construction of Industrial Internet Platform Test Bed of Quality inspection and analysis Project. The authors would like to thank the reviewers for their valuable and helpful comments, which have helped improved the paper considerably.

References

- [1] Makki Adham, Omer Siddig, Sabir Hisham. Advancements in hybrid photovoltaic systems for enhanced solar cells performance. *Renew Sustain Energy Rev* 2015; 2015(41):658–84.
- [2] Almonacid Florencia, Fernandez Eduardo F, Mellit Adel, Kalogirou Soteris. Review of techniques based on artificial neural networks for the electrical characterization of concentrator photovoltaic technology. *Renew Sustain Energy Rev* 2017; 75:938–53. [2017].
- [3] Sampaio Priscila Gonçalves Vasconcelos, González Mario Orestes Aguirre. Photovoltaic solar energy: conceptual framework. *Renew Sustain Energy Rev* 2017; 74:590–601.
- [4] M. Köntges, S. Kurtz, C. Packard, U. Jahn, K. Berger, K. Kato, T. Friesen, H. Liu, M. Van Iseghem, Review of Failures of Photovoltaic Modules, Technical Report, International Energy Agency, 2014.
- [5] O. Breitenstein, J. Bauer, K. Bothe, D. Hinken, J. Müller, W. Kwapil, M. C. Schubert, W. Warta, can luminescence imaging replace lock-in thermography on solar cells, *IEEE Journal of Photovoltaics* 1 (2011) 159–167. doi: 10.1109/JPHOTOV.2011.2169394.
- [6] Lécun Y, Bottou L, Bengio Y, et al. Gradient-based learning applied to document recognition [J]. *Proceedings of the IEEE*, 1998, 86(11):2278-2324.
- [7] Krizhevsky A, Sutskever I, Hinton G E. ImageNet classification with deep convolutional neural networks[C]// International Conference on Neural Information Processing Systems. Curran Associates Inc. 2012:1097-1105.
- [8] Szegedy C, Liu W, Jia Y, et al. Going deeper with convolutions[C]// IEEE Conference on Computer Vision and Pattern Recognition. IEEE, 2015:1-9.
- [9] G. O. Young, “Synthetic structure of industrial plastics,” in *Plastics*, 2nd ed., vol. 3, J. Peters, Ed. New York, NY, USA: McGraw-Hill, 1964, pp. 15–64.
- [10] W.-K. Chen, *Linear Networks and Systems*. Belmont, CA, USA: Wadsworth, 1993, pp. 123–135.
- [11] C. Cortes, V. Vapnik, Support-vector networks, *Machine Learning* 20 (1995) 273–297.
- [12] R.-E. Fan, K.-W. Chang, C.-J. Hsieh, X.-R. Wang, C.-J. Lin, Liblinear: A library for large linear classification, *The Journal of Machine Learning Research* 9 (2008)1871–1874.
- [13] C.-C. Chang, C.-J. Lin, LibSVM: A library for support vector machines, *ACM Transactions on Intelligent Systems and Technology* 2 (2011) 27:1–27:27.
- [14] K. Simonyan, A. Zisserman, Very Deep Convolutional Networks for Large-Scale Image Recognition, e-print,arXiv, 2014. ArXiv: 1409-1556.
- [15] J. Deng, W. Dong, R. Socher, L.-J. Li, K. Li, L. Fei-Fei. ImageNet: A large-scale hierarchical image database, in: *Conference on Computer Vision and Pattern Recognition (CVPR)*, 2009, pp. 248–255 M. Lin, Q. Chen, S. Yan, Network In Network, e-print,arXiv, 2013. arXiv:1312.4400.
- [16] M. Lin, Q. Chen, S. Yan, Network in Network, e-print, arXiv, 2013. arXiv:1312.4400.
- [17] D. P. Kingma, J. Ba, Adam: A Method for Stochastic Optimization, e-print, arXiv, 2014. arXiv:1412.6980.
- [18] M. Abadi, A. Agarwal, P. Barham, E. Brevdo, Z. Chen, C. Citro, G. S. Corrado, A. Davis, J. Dean, M. Devin, S. Ghemawat, I. Goodfellow, A. Harp, G. Irving, M. Isard, Y. Jia, R. Jozefowicz, L. Kaiser, M. Kudlur, J. Levenberg, D. Mané, R. Monga, S. Moore, D. Murray, C. Olah, M. Schuster,

J. Shlens, B. Steiner, I. Sutskever, K. Talwar, P. Tucker, V. Vanhoucke, V. Vasudevan, F. Viégas, O. Vinyals, P. Warden, M. Wattenberg, M. Wicke, Y. Yu, X. Zheng, TensorFlow: Large-scale machine learning on heterogeneous systems, 2015. URL: <https://www.tensorflow.org>.